COMMUNICATION

Direct observation of arene···sulphur dioxide interaction: Role of metal ions in electronic modulation for binding and activation

Received 00th January 20xx,
Accepted 00th January 20xx

DOI: 10.1039/x0xx00000x

Sandhya Singh,[a] Shruthi Dinesh,[a] Archana Yadav,[a] Sakthi Raje,[a] Ray J. Butcher,[b] Mahesh Sundararajan*[c] and Raja Angamuthu*[ad]

In the quest to understand ~~bioinspired~~ biologically relevant interactions of environmentally detrimental SO_2 with host molecules to modulate the electronic properties of the binding sites, we have directly observed the lone pair···π interaction between the aromatic ring and nucleophilic O of SO_2 (3.11 Å) for the first time in addition to the interaction between electrophilic S of SO_2 and metal bound thiolate (2.63 Å).

Sequestration and activation of SO_2 is topical owing to its industrial and environmental importance.[1] SO_2 is one among the environmental pollutants; it causes acid rain that poses risk to the marble/chalk exteriors of monumental structures (Taj Mahal, Mayan temples) and coral reefs by flaking them out into water-soluble form ($CaCO_3 + H_2SO_4 \rightleftharpoons CaSO_4 + CO_2 + H_2O$). Respiratory problems are triggered by SO_2-enriched air in megacities and areas around petrochemical industries. According to the World Health Organization (WHO),[2] SO_2 is one of the most dangerous air pollutants, with detrimental effects on health that are mainly associated with serious respiratory system alterations. As a result, there is a lot of interest in technologies that can capture SO_2 at the source of emission and turn it into valuable commodities.

SO_2 is known to interact with electron-rich centres of low-valent transition metal complexes ($M\cdots SO_2$),[3-5] anions such as sulfate,[6] high-valent metal centres ($M{-}OSO$),[7] heterocyclic compounds such as DABCO ($N\cdots SO_2$),[8] ionic liquids ($N^-\cdots SO_2$),[9-12] metal-bound thiolates ($MS^-\cdots SO_2$)[13,14] metal bound sulphides ($M_2S\cdots SO_2$),[15] metal-bound iodide ($M_2I\cdots SO_2$),[16] N-heterocyclic carbenes ($C\cdots SO_2$),[17] and phosphines ($R_3P\cdots SO_2$)[18] owing to its inherent polarity ($O{=}S^+{-}O^- \leftrightarrow O^-{-}S^+{=}O \leftrightarrow O^{0.5-}{-}S^+{-}O^{0.5-}$). Stoichiometric insertion of SO_2 into M-C bonds,[19-21] M-O bonds,[22,23] M-M bonds,[19,24] and P-B bonds[25] are also reported in the literature. Precise binding and visualisation of SO_2 onto hydroxy ($Al{-}OH\cdots O^{0.5-}{-}S^+{-}O^{0.5-}$)[26] and fluoride sites ($F\cdots SO_2$)[27] in metal-organic-frameworks[28] are also known.

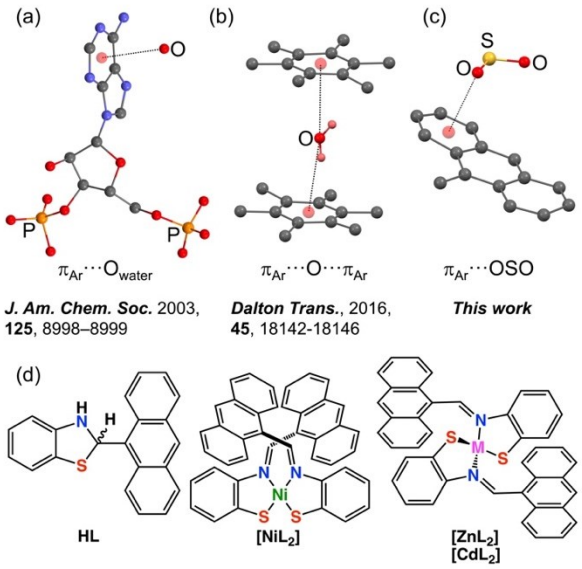

Figure. 1. (a) Lone pair···π interactions observed in the RNA pseudoknot[29] of beet western yellow virus;[30] (b) benzene–H_2O–benzene observed in a metal-organic framework;[31] (c) $Ar\cdots O_{SO_2}$ observed in the present study; (d) H-L and $[ML_2]$ where M is Ni, Zn or Cd are discussed in this work.

Our laboratory employed metal hydrides,[32] organic hydrides such as dihydrobenzimidazoles[33] or dihydrobenzothiazoles,[34] and redox active metal centres[35] to activate SO_2. Our goal is to sequester detrimental gases such as CO_2, SO_2, and halocarbons[36] utilising the weakest possible interactions so that the energy invested to release them from the host material is

[a] *Department of Chemistry, Indian Institute of Technology Kanpur, Kanpur 208016, India. raja@iitk.ac.in*
[b] *Department of Chemistry, Howard University, Washington, D.C. 20059, United States.*
[c] *Theoretical Chemistry Section, Chemistry Division, Bhabha Atomic Research Centre, Mumbai-400085, India; Homi Bhabha National Institute, Mumbai – 400 085, India.*
[d] *Department of Sustainable Energy Engineering, Kotak School of Sustainability, Indian Institute of Technology Kanpur, Kanpur 208016, India.*
† Footnotes relating to the title and/or authors should appear here.
Electronic Supplementary Information (ESI) available: [details of any supplementary information available should be included here]. See DOI: 10.1039/x0xx00000x

minimal. We have stumbled upon lone pair···π interaction as a perfect biologically relevant weak interaction to be explored. We have noticed that such interactions are ubiquitous in nature[29,30] and man-made molecular systems (Figure 1).[31] For example, the lone pair···π interaction between a nucleobase and water observed in the RNA pseudoknot[29] of beet western yellow virus[30] and in between an arene ring and water in the metal-organic framework[31] is appealing. The anthracenyl substituted dihydrobenzothiazole (HL) was chosen for the present study due to its bright colour and, for the possibility of aforementioned ~~bioinspired~~ weak interactions and, its ability to function as an organic hydride donor in small molecule activation.[34,37-39] Square–planar enforcing nickel(II) ion and tetrahedral enforcing zinc(II) and cadmium(II) ions were chosen to modulate the electronic properties of the metal-bound thiolate in the binding or activation of SO_2.

The benzothiazoline, 2-(9-anthracenyl)-2,3-dihydrobenzothiazole (HL), was prepared through a simple reaction between 9-anthracenecarboxaldehyde and 2-aminothiophenol in ethanol under nitrogen atmosphere. The bright yellow, air-sensitive solid was characterised by electrospray ionisation mass spectrometry (ESI-MS), ^1H and ^{13}C NMR. (Fig. S1-S4).[34,37-39] A dichloromethane solution of HL in an inert atmosphere was saturated with dry SO_2 and opened to air, which changed the colour of the solution from yellow to red (Scheme 1). The ESI-MS analysis of an aliquot of the red solution was performed. The positive ion ESI-MS showed a prominent envelope centred at 312.0848 confirming the presence of 2-(anthracen-9-yl)benzothiazolium cation (calcd. 312.0847) whereas the negative ion ESI-MS (Fig. S5-S8) had an envelope at 96.9598 confirming the presence of bisulphate anion (calcd. 96.9596). This reactivity aligns with our previous reports on SO_2 activation by benzothiazolines[34,35] and benzimidazolines.[33]

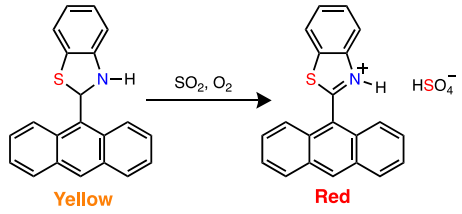

Scheme 1. Formation of 2-(anthracen-9-yl)benzothiazolium bisulphate from 2-(9-anthracenyl)-2,3-dihydrobenzothiazole (HL) upon interaction with SO_2.

The reaction of HL with 0.5 equivalent of $Ni(OAc)_2{\cdot}4H_2O$ yielded NiL_2 in good yield. Dark brown needles of $[NiL_2]$ suitable for single crystal X-ray diffraction (SCXRD) analysis were obtained by layering of $CHCl_3$ on a methanolic solution; crystallographic and refinement data are provided in Table S1. A projection of the molecular structure is given in Fig. 2 with selected bond distances and angles. The Ni(II) centre has considerable tetrahedral distortion with a dihedral angle of 9.92° (between the triangular planes N1Ni1S1 and N2Ni1S2). The bidentate imine-thiolate ligands are cis-enforced due to the presence of three intramolecular π···π interactions (3.62 Å, 3.87 Å, 3.92 Å) whereas similar bidentate ligands comprising strong-field donors coordinated to low-spin Ni(II) centres with a trans orientation of the ligands.[40]

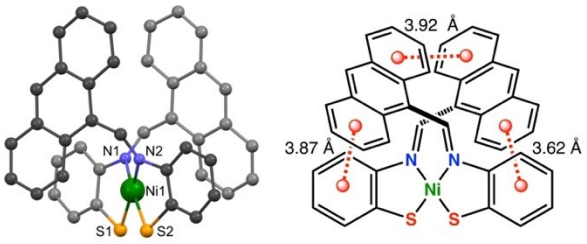

Figure. 2. Solid-state structure of $[NiL_2]{\cdot}2CHCl_3$. Solvents are omitted for clarity. Selected distances [Å] and angles [°]: Ni(1)-S(1), 2.187(2); Ni(1)-S(2), 2.186(2); Ni(1)-N(2), 1.930(5); Ni(1)-N(1), 1.914(6); S(2)-Ni(1)-S(1), 87.19(8); N(2)-Ni(1)-S(1), 171.70(16); N(2)-Ni(1)-S(2), 86.54(17); N(1)-Ni(1)-S(1), 87.24(17); N(1)-Ni(1)-S(2), 170.51(17); N(1)-Ni(1)-N(2), 99.9(2) (CCDC 2348655).

Purging SO_2 gas to a brown solution of $[NiL_2]$ in dichloromethane changed the colour to red which yielded diffraction-quality red colour crystals. The SCXRD analysis provided the solid-state structure where an SO_2 was seen interacting with a thiolate sulphur of $[NiL_2]$ (Fig. 3) through $S_{SO_2}\cdots S_{thiolate}$ connection; the observed $S^{-}\cdots SO_2$ distance of 2.63 Å is well below the sum of the van der Waals radii (S + S = 3.6 Å).[41] Whereas another SO_2 present in the lattice is interestingly utilising lone-pair···π interaction between one of the aromatic rings of anthracenyl moiety and O of SO_2 with a distance of 3.11 Å. To the best of our knowledge, this snapshot of SO_2 located on top of an aromatic ring through lone pair···π interaction between the electron-rich O of SO_2 ($O^{\delta-}=S^{\delta+}=O^{\delta-}$) and the electron-poor centroid of anthracenyl moiety is the first known example of this sort. However, contact between electrophilic S of SO_2 and metal-bound thiolate is known in literature reports of Darensbourg.[13,14] Other features such as cis-enforcement of the bidentate imine-thiolate ligands due to the presence of intramolecular π···π interactions (3.59 Å, 3.82 Å) are similar to $[NiL_2]$. The Ni(II) centre has more tetrahedral distortion with a dihedral angle of 24° (between the triangular planes N1Ni1S1 and N2Ni1S2) compared to $[NiL_2]$.

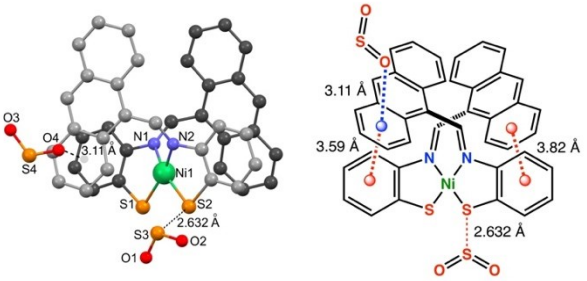

Figure. 3. Solid-state structure of $[NiL_2]{\cdot}2SO_2$ showing the SO_2 interactions with $[NiL_2]$ through $S_{SO_2}\cdots S_{thiolate}$ and $O_{SO_2}\cdots Ar_{anthracenyl}$ (lone-pair···π) contacts. Selected distances [Å] and angles [°]: Ni(1)-S(1), 2.1791(5); Ni(1)-S(2), 2.1840(6); Ni(1)-N(2), 1.9231(16); Ni(1)-N(1), 1.9037(16); S(3)-O(1), 1.4358(18); S(3)-O(2), 1.4371(18); S(4)-O(3), 1.408(2); S(4)-O(4), 1.396(2); S(1)-Ni(1)-S(2), 94.05(2); N(1)-Ni(1)-S(1), 87.28(5); N(1)-Ni(1)-S(2), 162.03(6); N(1)-Ni(1)-N(2), 95.90(7); N(2)-Ni(1)-S(1), 164.93(5); N(2)-Ni(1)-S(2), 87.46(5); O(1)-S(3)-O(2), 115.86(12); O(4)-S(4)-O(3), 117.23(17) (CCDC 2348656).

The thermogravimetric analysis of $[NiL_2]\cdot 2SO_2$ revealed that the SO_2 molecules are retained in the lattice till ~110 °C (Fig. S28). It is noteworthy that the $[NiL_2]$ has thermal stability up to ~350 °C; this means that the $[NiL_2]$ could be used as solid-state scrubber in the industries where SO_2 is a gaseous waste that are emitted at temperatures higher than room temperature.

To evaluate the electronic modulations on the metal-bound thiolate as it is a site for SO_2 binding, we have synthesised $[ZnL_2]$ and $[CdL_2]$ complexes (Fig. 4). We have anticipated higher electron density on sulphur in the ionic-like tetrahedral Zn- and Cd-complexes with respect to the more covalent character of the Ni-S bond in square-planar $[NiL_2]$. The $[ZnL_2]$ complex was maroon in colour and $[CdL_2]$ was coffee brown due to ligand-to-metal charge transfer. Both the complexes possessed considerable distortion from tetrahedral geometry (Zn, 82.73° and Cd, 84.01°) due to the intermolecular π···π interactions (Zn, 3.69 and 3.63 Å; Cd, 3.71 and 3.66 Å).

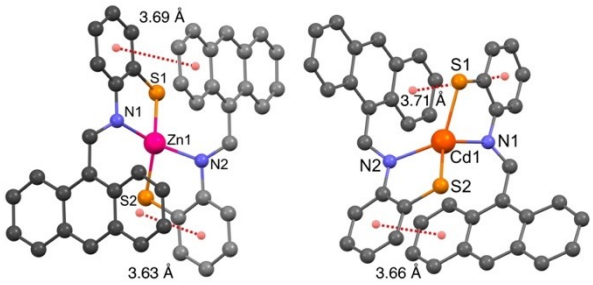

Figure 4. Selected distances [Å] and angles [°] for $[ZnL_2]\cdot 2CHCl_3$: Zn(1)-S(1), 2.2764(11); Zn(1)-S(2), 2.2751(10); Zn(1)-N(2), 2.080(3); Zn(1)-N(1), 2.087(3); S(2)-Zn(1)-S(1), 129.04(4); N(2)-Zn(1)-S(2), 88.01(9); N(2)-Zn(1)-S(1), 118.32(9); N(1)-Zn(1)-S(2), 116.19(9); N(1)-Zn(1)-S(1), 87.34(9); N(1)-Zn(1)-N(2), 121.93(12) (CCDC 2348657). Selected distances [Å] and angles [°] for $[CdL_2]_3\cdot 2(C_2H_5)_2O$: Cd(1)-S(1), 2.4432(7); Cd(1)-S(2), 2.4403(7); Cd(1)-N(2), 2.306(2); Cd(1)-N(1), 2.336(2); S(2)-Cd(1)-S(1), 132.66(2); N(2)-Cd(1)-S(2), 81.77(5); N(2)-Cd(1)-S(1), 125.17(5); N(1)-Cd(1)-S(2), 118.32(6); N(1)-Cd(1)-S(1), 81.08(6); N(2)-Cd(1)-N(1), 123.66(7) (CCDC 2348658). Only $[ZnL_2]$ and $[CdL_2]$ are shown for the sake of clarity.

The SO_2 saturated solutions of $[ZnL_2]$ and $[CdL_2]$ complexes were left to stand in open air; ESI-MS analysis indicated the presence of benzothiazolium and bisulfate ions in both cases in line with our previous results (Scheme 2; Fig. S13-S21).[34] This reactivity suggests that the thiolates of $[NiL_2]$ possess electron density just enough to bind with SO_2. In contrast, the thiolates of $[ZnL_2]$ and $[CdL_2]$ possess stronger electron density that they can activate the SO_2 into sulphate. To understand this further we have employed density functional theory.

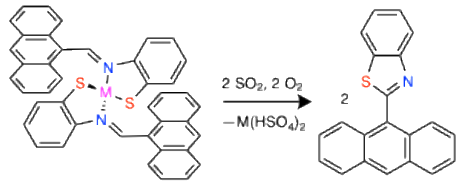

Scheme 2. The interaction of $[ZnL_2]$ and $[CdL_2]$ complexes with SO_2 in the presence of air.

The three transition metal complexes presented can just bind with SO_2 or activate it further. This is primarily determined by the type of central metal ion and the geometry of the complex, which in turn governs the available electron density on the metal-bound thiolates. All three complexes are in divalent oxidation state with S = 0 (low) spin states and the reason behind the small molecule binding/activation is intriguing. It can be supported by carrying out electronic structure calculations (B3LYP/D3BJ-def2-TZVP). The technical details of the simulations are given in the supporting information. The optimised structural parameters of $[NiL_2]$, $[ZnL_2]$ and $[CdL_2]$ complexes are in line with the same from the experimental solid-state structures within 0.1 Å for all three species. Between the TM-N and TM-S bond lengths, the latter ones are excellently reproduced within 0.03 Å as shown in Figure 5. As expected, the d^8 $[NiL_2]$ complex favours the square-planar geometry, whereas the d^{10} Zn(II) and Cd(II) complexes favour the tetrahedral geometry as indicative from their bond angles.

Further, the thiolate charges play a vital role in the binding and activating of the SO_2 molecule. The charge on the thiolates increases drastically from Ni to Cd species as shown in Figure 5. This is crucial for the initial binding of SO_2. We note that Ni-S bond is more covalent leading to the formation of a short Ni–S bond, whereas in Zn and Cd-complexes, the filled d-orbitals favour tetrahedral coordination. For instance, the charges on Ni(II), Zn(II) and Cd(II) ions are 0.022, 0.429 and 0.819 au respectively which indicate the dominant covalent nature of Ni-complex, whereas an ionic bonding for the Zn and Cd-species. The more ionic bonding in Zn- and Cd-complexes will favour ligand dissociation upon reacting with SO_2 leading to the formation of 2-(anthracen-9-yl)benzothiazolium bisulphate.

We have calculated the structures and binding energies of SO_2 to the NiL_2 complex. The computed structures and energies are shown in Figure S34. We have calculated the structures individually on the arene site and at the thiolate site in 1:1 and 1:2 ratios. As expected, the SO_2 binding is favourable at the thiolate site by ~4 kcal/mol compared to the arene site in both 1:1 and 1:2 ratios. The S···S bond length is ~ 2.80 Å which is shorter compared to ~3.01 Å in the arene site. The computed binding energies are typical for such weak van der Waals interactions as reported in the literature.[42,43] Thus, due to a minor difference in binding energies, it is unlikely to see two different peaks in TGA for SO_2 dissociation.

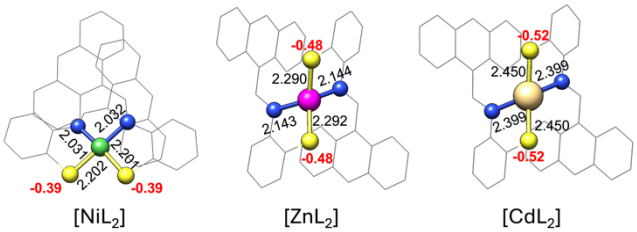

Figure 5. Optimized structures with selected bond distances (in Å) and Mulliken charges on thiolates (in a.u). Ni, green; Zn, magenta; Cd, sandal; C, grey. Hydrogens are omitted for the sake of clarity.

In summary, we report the first example of arene···OSO lone pair···π interaction in addition to the interaction between

electrophilic S of SO_2 and metal-bound thiolate. We observed changes in the available electron density on the metal-bound thiolates upon binding to selected metal ions that in turn dictated the binding ($[NiL_2]$) or activation of SO_2 into sulphate ($[ZnL_2]$ and $[CdL_2]$). Our ongoing efforts are dedicated to modulating the electronic properties of the arene rings of the host materials to sequester detrimental molecules.

The financial support was from the Ministry of Earth Sciences, India (MOES/CCR/PALEO-08/2015) and the Science and Engineering Research Board, India (CRG/2020/ 001708). For Senior Research Fellowships, SS and SR thank the Council of Scientific and Industrial Research, India, and SD thanks the Ministry of Education, India. SD and AY are recipients of the Prime Minister's Research Fellowship.

Data Availability

The data for this manuscript can be found at https://doi.org/10.15124/. This includes synthesis, NMR, mass, X-ray, UV-Vis and DFT details.

Conflicts of interest

There are no conflicts to declare.

Notes and references

1. X. Han, S. Yang and M. Schröder, *Nat. Rev. Chem.*, 2019, **3**, 108-118.
2. WHO, *Air quality guidelines: Global update 2005: Particulate matter, ozone, nitrogen dioxide, and sulfur dioxide*, World Health Organization, 2006.
3. Z. Arcís-Castillo, F. J. Muñoz-Lara, M. C. Muñoz, D. Aravena, A. B. Gaspar, J. F. Sánchez-Royo, E. Ruiz, M. Ohba, R. Matsuda, S. Kitagawa and J. A. Real, *Inorg. Chem.*, 2013, **52**, 12777-12783.
4. M. Albrecht, R. A. Gossage, M. Lutz, A. L. Spek and G. van Koten, *Chem. Eur. J.*, 2000, **6**, 1431-1445.
5. R. Mews, E. Lork, P. G. Watson and B. Görtler, *Coord. Chem. Rev.*, 2000, **197**, 277-320.
6. P. Bruna, A. Decken, F. Grein, J. Passmore, J. M. Rautiainen, S. Richardson and T. Whidden, *Inorg. Chem.*, 2013, **52**, 7193-7202.
7. E. Solari, C. Floriani and K. Schenkb, *Chem. Comm.*, 1990, 963-964.
8. H. Woolven, C. González-Rodríguez, I. Marco, A. L. Thompson and M. C. Willis, *Org. Lett.*, 2011, **13**, 4876-4878.
9. Z. Wang and D. Yang, *Chem. Comm.*, 2022, **58**, 6212-6214.
10. G. Cui, F. Zhang, X. Zhou, H. Li, J. Wang and C. Wang, *Chem. Eur. J.*, 2015, **21**, 5632-5639.
11. G. Cui, F. Zhang, X. Zhou, Y. Huang, X. Xuan and J. Wang, *ACS Sus. Chem. Eng.*, 2015, **3**, 2264-2270.
12. D. Yang, M. Hou, H. Ning, J. Ma, X. Kang, J. Zhang and B. Han, *ChemSusChem*, 2013, 1191-1195.
13. M. L. Golden, J. C. Yarbrough, J. H. Reibenspies and M. Y. Darensbourg, *Inorg. Chem.*, 2004, **43**, 4702-4707.
14. M. Y. Darensbourg, T. Tuntulani and J. H. Reibenspies, *Inorg. Chem.*, 1995, **34**, 6287-6294.
15. G. J. Kubas, H. J. Wasserman and R. R. Ryan, *Organometallics*, 1985, **4**, 419-421.
16. P. G. Eller, G. J. Kubas and R. R. Ryan, *Inorg. Chem.*, 1977, **16**, 2454-2462.
17. Michael K. Denk, K. Hatano and Alan J. Lough, *Eur. J. Inorg. Chem.*, 2002, **2003**, 224-231.
18. F. Buss, P. Rotering, C. Muck-Lichtenfeld and F. Dielmann, *Dalton Trans*, 2018, **47**, 10420-10424.
19. R. P. Kelly, N. Kazeminejad, C. A. Lamsfus, L. Maron and P. W. Roesky, *Chem. Comm.*, 2016, **52**, 13090-13093.
20. B. Y. Lee, H. Y. Kwon, S. Y. Lee, S. J. Na, S.-i. Han, H. Yun, H. Lee and Y.-W. Park, *J. Am. Chem. Soc.*, 2005, **127**, 3031-3037.
21. R. Eberhardt, M. Allmendinger, G. A. Luinstra and B. Rieger, *Organometallics*, 2003, **22**, 211-214.
22. C. Schoo, S. V. Klementyeva, M. T. Gamer, S. N. Konchenko and P. W. Roesky, *Chem. Comm.*, 2016, **52**, 6654-6657.
23. A.-C. Schmidt, F. W. Heinemann, C. E. Kefalidis, L. Maron, P. W. Roesky and K. Meyer, *Chem. Eur. J.*, 2014, **20**, 13501-13506.
24. A. Noor, S. Qayyum, T. Bauer, S. Schwarz, B. Weber and R. Kempe, *Chem. Comm.*, 2014, **50**, 13127-13130.
25. N. Szynkiewicz, J. Chojnacki and R. Grubba, *Inorg. Chem.*, 2020, **59**, 6332-6337.
26. S. Yang, J. Sun, A. J. Ramirez-Cuesta, S. K. Callear, I. F. DavidWilliam, D. P. Anderson, R. Newby, A. J. Blake, J. E. Parker, C. C. Tang and M. Schröder, *Nat. Chem.*, 2012, **4**, 887-894.
27. M. R. Tchalala, P. M. Bhatt, K. N. Chappanda, S. R. Tavares, K. Adil, Y. Belmabkhout, A. Shkurenko, A. Cadiau, N. Heymans, G. De Weireld, G. Maurin, K. N. Salama and M. Eddaoudi, *Nat. Comm.*, 2019, **10**.
28. E. Martinez-Ahumada, D. He, V. Berryman, A. Lopez-Olvera, M. Hernandez, V. Jancik, V. Martis, M. A. Vera, E. Lima, D. J. Parker, A. I. Cooper, I. A. Ibarra and M. Liu, *Angew Chem Int Ed Engl*, 2021, **60**, 17556-17563.
29. S. Sarkhel, A. Rich and M. Egli, *J. Am. Chem. Soc.*, 2003, **125**, 8998-8999.
30. M. Egli, G. Minasov, L. Su and A. Rich, *Proceedings of the National Academy of Sciences of the United States of America*, 2002, **99**, 4302-4307.
31. X.-Y. Dong, X. Li, B. Li, Y.-Y. Zhu, S.-Q. Zang and M.-S. Tang, *Dalton Trans.*, 2016, **45**, 18142-18146.
32. S. Raje and R. Angamuthu, *Green Chem.*, 2019, **21**, 2752-2758.
33. S. Mehrotra, S. Raje, A. K. Jain and R. Angamuthu, *ACS Sus. Chem. Eng.*, 2017, **5**, 6322-6328.
34. S. Mehrotra, R. J. Butcher and R. Angamuthu, *ACS Sus. Chem. Eng.*, 2016, **4**, 6517−6523.
35. M. Chahal, S. Raje, G. Kotana and R. Angamuthu, *Green Chem.*, 2019, **21**, 6372-6380.
36. S. Vidal, *ACS Central Science*, 2020, **6**, 83-86.
37. K. H. Kim, T. Akiyama and C. H. Cheon, *Chem. Asian. J.*, 2016, **11**, 274-279.
38. C. Zhu, K. Saito, M. Yamanaka and T. Akiyama, *Acc. Chem. Res.*, 2015, **48**, 388-398.
39. C. Zhu and T. Akiyama, *Org. Lett.*, 2009, **11**, 4180-4183.
40. J. A. W. Verhagen, D. D. Ellis, M. Lutz, A. L. Spek and E. Bouwman, *J. Chem. Soc. Dalton Trans.*, 2002, 1275-1280.
41. T. J. Mooibroek, P. Gamez and J. Reedijk, *CrystEngComm*, 2008, **10**, 1501.
42. Y. Jin, W. Li, R. T. Saragi, M. Juanes, C. Pérez, A. Lesarri and G. Feng, *Phys. Chem. Chem. Phys.*, 2023, **25**, 12174-12181.
43. I. S. Antonijević, G. V. Janjić, M. K. Milčić and S. D. Zarić, *Cryst. Growth Des.*, 2016, **16**, 632-639.

